JOURNAL OF GEOPHYSICAL RESEARCH, VOL. 98, NO. C6, PAGES 10,271–10,278, JUNE 15, 1993

The Statistical Distribution of Swash Maxima on Natural Beaches

K.T. HOLLAND AND R.A. HOLMAN

College of Oceanic and Atmospheric Sciences, Oregon State University, Corvallis

Cartwright and Longuet-Higgins (1956) describe the statistical distribution of maxima that would result from the linear superposition of random, Gaussian waves. The distribution function depends solely upon the relative width of the power spectrum and root-mean-square value of the process time series. Runup field data from three experiments are presented to determine the extent to which the distribution of swash maxima can be approximated using the Cartwright and Longuet-Higgins probability density function. The model is found to be satisfactory for describing various distribution statistics including the average maxima, the proportion of negative maxima, and the elevation at which one third of the swash maxima are exceeded. However, systematic discrepancies that scale as a function of time series skewness are observed in the statistics describing the upper tail of the distributions. Although we conclude that the linear model is incapable of delineating these apparent nonlinearities in the swash time series, the extent of the deviation can be estimated empirically for the purpose of constraining nonlinear models and nearshore engineering design.

INTRODUCTION

Estimation of extreme values of wave runup (shoreline water level) is of interest to oceanographers, ocean engineers, and coastal planners. Many applications require accurate predictions of maximum runup elevations to allow choice of appropriate and economically feasible shoreline setback criteria and design of shore protection structures. Maximum runup prediction under monochromatic conditions is straightforward; the runup reaches approximately the same elevation for every wave. However, under random wave conditions, a distribution of runup maximum elevations is observed. In the following, we apply an existing statistical model to estimate the distribution of runup maxima under the assumption that runup can be approximated as a linear, Gaussian process.

Figure 1 diagrams a hypothetical runup time series. For a given set of wave conditions, the runup elevation $\eta(t)$ can be decomposed into two components. The setup, $\overline{\eta}$, is taken to be the mean water surface elevation above the still water level, while swash, $\eta'(t)$, is defined as fluctuations of the runup about the setup level, $\eta'(t) = \eta(t) - \overline{\eta}$. Laboratory researchers commonly use the term runup to describe discrete maximum elevations rather than a continuous process, and make no distinction between setup and swash. We would like to remove this ambiguity by defining swash maxima ζ to be the difference in elevation between any local crest in $\eta(t)$ and the setup level. Although this definition of local maxima is less common than the zero-crossing definition, R, the distribution of local maxima can be derived theoretically. One major difference between the two definitions of maxima is that for non-narrow-band processes the local maxima definition can be either positive or negative, while the zero-crossing definition allows for only positive maxima. Both definitions are equivalent for extremely narrow-band time series. For simplicity, subsequent use of the symbols defined above will pertain to nondimensional forms, whereas a caret (^) indicates specific reference to physical variables.

Theories describing the swash motions of irregular, breaking waves (reviewed by *LeMéhauté et al.* [1968]) are difficult to apply to field and laboratory data. However, several empirical methods for determining the distribution of irregular wave runup maxima have been formulated. One of the earliest methods, given by *Saville* [1962], relies on individual wave analysis to construct the runup maxima distribution. Basically, a runup relation developed under monochromatic wave conditions is applied to equivalent individual waves from an irregular wave train. The assumption inherent to this method is known as the hypothesis of equivalency. Equivalency is not an assumption of linearity in terms of direct superposition; rather, the hypothesis presumes linear relationships between statistical averages only, not individuals. The resulting empirical distribution is calculated graphically for each particular combination of wave steepness and structure slope assuming independence of deepwater wave height and length. *Battjes* [1971] extended Saville's method to include conditions of varying correlation between wavelength and wave height by making the additional assumption that the maximum monochromatic runup elevation, $\hat{R}$, is given by *Hunt*'s [1959] empirical equation for waves breaking on a smooth slope:

$$\hat{R} = C\sqrt{\hat{H}_0 \hat{L}_0}\tan\beta \tag{1}$$

where $\hat{H}_0$ is the offshore wave height, $\hat{L}_0$ is the offshore wavelength, $\tan\beta$ is the beach slope, and C is an empirical constant.

Since there is no equivalent offshore wave, the hypothesis of equivalency used in these linear models is inappropriate for conditions of significant infragravity (low frequency) energy, commonly a dominant component of field runup signals [*Guza and Thornton*, 1982]. Although other theoretical runup distribution models have been proposed [*Ahrens*, 1979, 1983; *Nielsen and Hanslow*, 1991; *Sawaragi and Iwata*, 1984], they either depend upon equivalency or rely upon empirical "weighting" coefficients that obscure the physics of their development. In addition, the zero-crossing definition of runup maxima used in all of these models should most properly be restricted to describing very narrow-banded spectra. This definition is incapable of distinguishing the differences from broad-banded forms and is therefore inappropriate for use as a generic descriptor of process maxima. Finally, most of the previous models have been largely unconstrained by field data.

Paper number 93JC00035.
0148-0227/93/93JC-00035$05.00

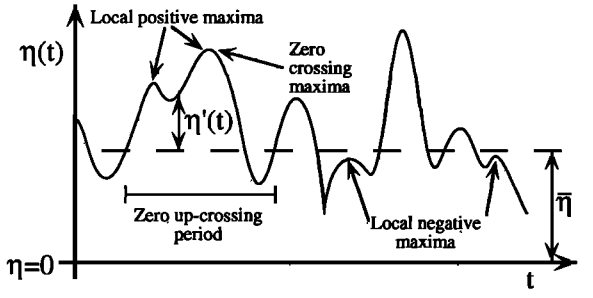

Fig. 1. Definition diagram of runup variables.

Our principle objective is to characterize the wave runup maxima probability density function (pdf) for field data in terms of a model that does not assume equivalency, but still has a physical basis. In the following, we describe a probabilistic model for the local maxima of an arbitrary Gaussian process in which the form of the pdf is provided completely by its energy spectrum. The model is then tested with runup data from three separate field sites taken under a variety of environmental conditions. Finally, deviation from the predictions is shown to be a function of nonlinearity in the runup time series.

Statistical Model Application

Following *Rice* [1944, 1945], *Cartwright and Longuet-Higgins* [1956] (hereinafter referred to as CLH56) present the theoretical, statistical distribution of maxima of an arbitrary stochastic function, $f(t)$, formed as the sum of an infinite number of sine waves of random phase and zero mean:

$$f(t) = \sum_{n}^{\infty} c_n \cos(\sigma_n t + \phi_n) \tag{2}$$

where the frequencies, σ_n, are distributed densely in the interval $(0,\infty)$, the phases, ϕ_n, are uniformly distributed between 0 and 2π, and the amplitudes, c_n, are given by the energy spectrum. Through application of the central limit theorem $f(t)$ can be shown to be a Gaussian process with a pdf given by the Gaussian (or standard normal) distribution. Although not all Gaussian processes are necessarily linear, it is common to approximate random processes using linear superposition as given by equation (2).

The pdf of the normalized maxima, $\zeta = \hat{\zeta}/\sqrt{m_0}$ of $f(t)$ is given by CLH56:

$$p(\zeta) = \frac{1}{\sqrt{2\pi}}\left[\varepsilon e^{-\frac{1}{2}\zeta^2/\varepsilon^2} + \sqrt{1-\varepsilon^2}\,\zeta e^{-\frac{1}{2}\zeta^2}\int_{-\infty}^{\zeta\sqrt{1-\varepsilon^2}/\varepsilon} e^{-\frac{1}{2}x^2}dx\right] \tag{3}$$

Thus the distribution of maxima will depend on only two parameters: a normalization factor, $\sqrt{m_0}$, which is the root-mean-square of $f(t)$, and the "spectral width" parameter, ε, which represents the relative width of the energy density spectrum, $E(\sigma)$, of $f(t)$:

$$\varepsilon^2 = \frac{m_0 m_4 - m_2^2}{m_0 m_4} \qquad m_n = \int_0^{\infty} E(\sigma)\sigma^n d\sigma \tag{4}$$

Figure 2 shows the range of maxima distributions as a function of the spectral width parameter ε. We note that for an infinitely narrow spectrum ($\varepsilon \to 0$) (where the zero-crossing and local maximum definitions are equivalent) the distribution of normalized maxima, ζ, is given by the Rayleigh distribution:

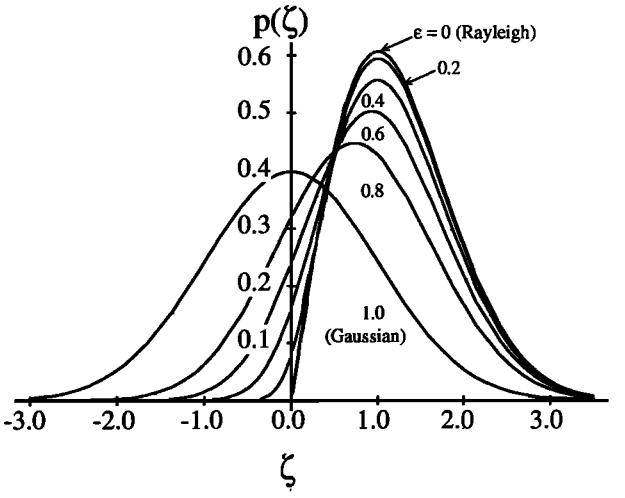

Fig. 2. Statistical distribution of maxima of a random process as a function of the spectral width parameter, ε [after *Cartwright and Longuet-Higgins*, 1956]. As ε increases, the proportion of negative maxima increases, while the mean and the mode decrease.

$$p(\zeta) = \begin{cases} \zeta e^{-\frac{1}{2}\zeta^2} & (\zeta \geq 0) \\ 0 & (\zeta < 0) \end{cases} \tag{5}$$

As ε approaches its maximum value of 1, the distribution of ζ tends to a Gaussian distribution with zero mean and standard deviation equal to 1

$$p(\zeta) = \frac{1}{\sqrt{2\pi}} e^{-\frac{1}{2}\zeta^2} \tag{6}$$

Note that as the spectral width increases, changes in the following distribution statistics result: the proportion of negative maxima increases, while the mean, the mode, and the skewness of $p(\zeta)$ decrease.

It may be somewhat surprising that we are attempting to describe swash motions using a linear model given the strong nonlinearities that are common in the nearshore zone. However, linear models have had considerable success in describing swash dynamics [*Miche*, 1951; *Suhayda*, 1974]. In fact, the nonlinear, finite amplitude development of *Carrier and Greenspan* [1958] shows that under certain conditions the amplitude of the swash motion does not differ from that given by linear theory. Additionally, wave kinematics [*Guza and Thornton*, 1980] and phase velocity [*Thornton and Guza*, 1982] observations have been shown to be consistent with linear theory in a region well beyond its theoretically applicable range. Therefore extension of linear-based hypotheses to describe swash maxima deserves consideration.

Field Measurements

The model was tested over a range of model parameters using results from three experiments: the Louisiana Barrier Island Erosion Study (LBIES) [*Sallenger et al.*, 1987], the joint University SWASH (USWASH) experiment, and the Duck Experiment on Low-frequency and Incident-band Longshore

TABLE 1. Ranges of Environmental Conditions at the Different Experiment Locations

Experiment	Dates	Location	Method	Number of Runs	Hs, m	T, s	tan β
LBIES	Feb. 14–25, 1989	Isles Dernieres, La	Wire	67	0.58–0.87	4.0–6.0	0.05
USWASH	Jun. 26–29, 1989	La Jolla, Calif	Video	2	0.54–2.35	5.8–13.6	0.03
DELILAH	Oct. 3–19, 1990	Duck, N.C.	Video	16	0.94–2.71	5.1–10.2	0.07

and Across-shore Hydrodynamics (DELILAH) [*Birkemeier et al.*, 1991] experiment. To our knowledge, this work incorporates one of the largest and most accurate field runup data sets ever collected.

As part of the LBIES, an experiment took place on the barrier island of Isles Dernieres, Louisiana, and was designed to track the propagation of runup and overwash bores over low-lying topography. During this experiment, a resistance wire runup sensor provided runup data between February 14 and 25, 1989. The USWASH experiment was conducted over a 4-day period at Scripps Beach in La Jolla, California, during June 1989. The objective of this experiment was to accurately sample swash processes using various methods. Both video-based and resistance wire runup sensors were deployed. However, only the video results will be presented in the model application. DELILAH was a multi-investigator study of nearshore dynamics on a barred beach, including the response of sand bars to waves. The experiment was located at the U.S. Army Corps of Engineers Field Research Facility in Duck, North Carolina. Over a 3-week period in October 1990, swash zone video recordings were made almost continuously during daylight hours.

The environmental conditions and beach types varied substantially among the three experiment locations (Table 1). The data cover conditions ranging from incident (typical period O(10) seconds) to infragravity (period 20–300 s) energy dominated conditions, representing a variety of combinations of sea and swell. Offshore significant wave heights varied from 0.54 to 2.71 m, with peak periods between 4 and 13 s. Approximate foreshore profile slopes defined over the swash region ranged from 1:33 to 1:15.

The video recordings from USWASH and DELILAH were analyzed using a modified version of the "timestack" method described by *Aagaard and Holm* [1989]. For each specific camera view, the screen locations of a measured, shore-normal, beach profile (extending from the dry beach across the swash region) were computed using known geometric transformations [*Lippmann and Holman*, 1989]. An image-processing system was used to digitize picture element (pixel) intensities along the cross-shore transect and then rewrite the intensities horizontally across a separate (initially empty) frame buffer. Subsequent samplings (at a constant time interval) of transect pixels were "stacked" down the frame buffer such that cross-shore distance is represented along the horizontal axis, and

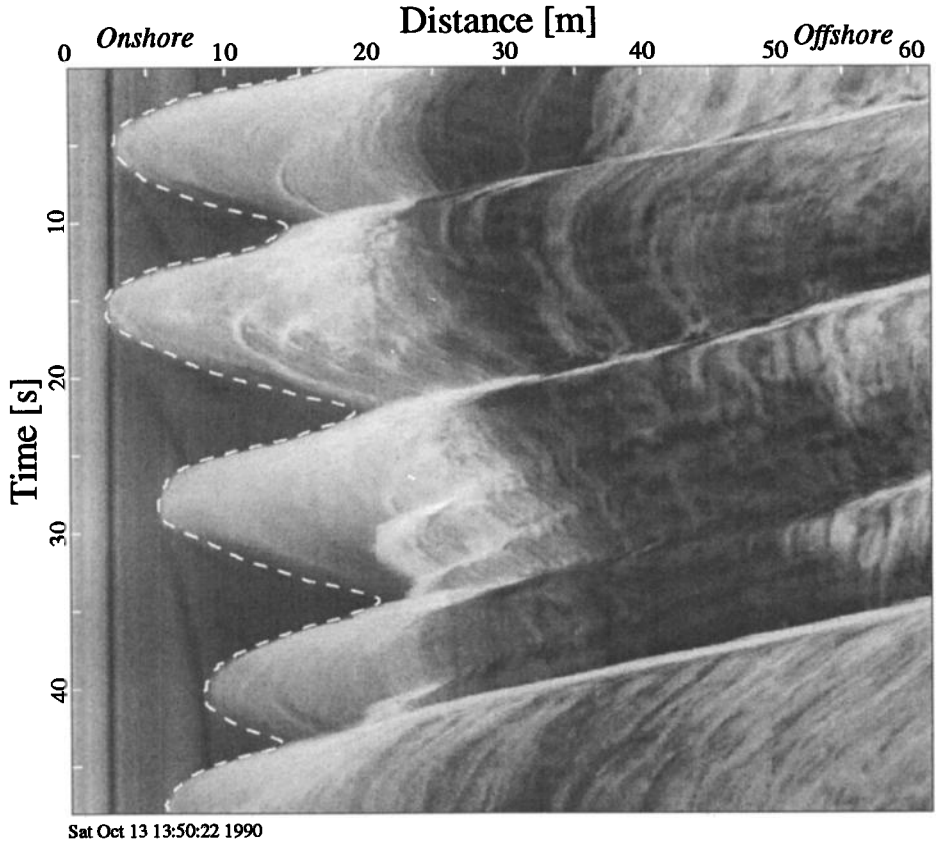

Fig. 3. "Timestack" from the DELILAH experiment showing the cross-shore location of the runup edge (dashed line) over time. The intensity patterns seaward of the runup edge reflect changes in the flow field at greater depths. The slope of the approximately linear features represents the speed of incoming runup bores.

time increases down the screen. In this manner, timestacks provide visual information of the cross-shore variability of pixel intensity over time.

A typical timestack is shown in Figure 3. The position of the swash edge can be visually identified by the sharp change in intensity between the darker beach surface and the lighter "foamy" edge of the swash bore. Swash edge detection (shown by the dashed line) was accomplished using standard image-processing algorithms along with manual refinements. The appropriate inverse transformation to ground coordinates allowed computation of swash elevations. The vertical resolution of this technique for these experiments ranged between 1 and 4 cm.

The runup sensor measurements made during the LBIES utilized a dual wire resistance gauge (described by *Guza and Thornton* [1982]) deployed horizontally across the beach at a height, δ, above the sand surface. Accuracies and resolutions of this method as compared with the video measurements have been discussed previously [*Holman and Guza*, 1984], and are not extended here. However, it is noted that comparisons between the two methods [*Holland and Holman*, 1991] suggest that as $\delta \rightarrow 0$, the wire measurements approach the video results (for the LBIES deployment, δ = 4 cm). Any significant discrepancies between methods are expected to be apparent only with regard to mean and variance values and not with regard to the distribution shapes.

Data were selected for analysis based on an assessment of the performance of the timestack and runup wire methods. Those video records having very low-intensity contrast between beach and the swash (and therefore a larger probability of estimation error) were eliminated. Similarly, wire data runs were also excluded whenever the sensor was fouled by debris.

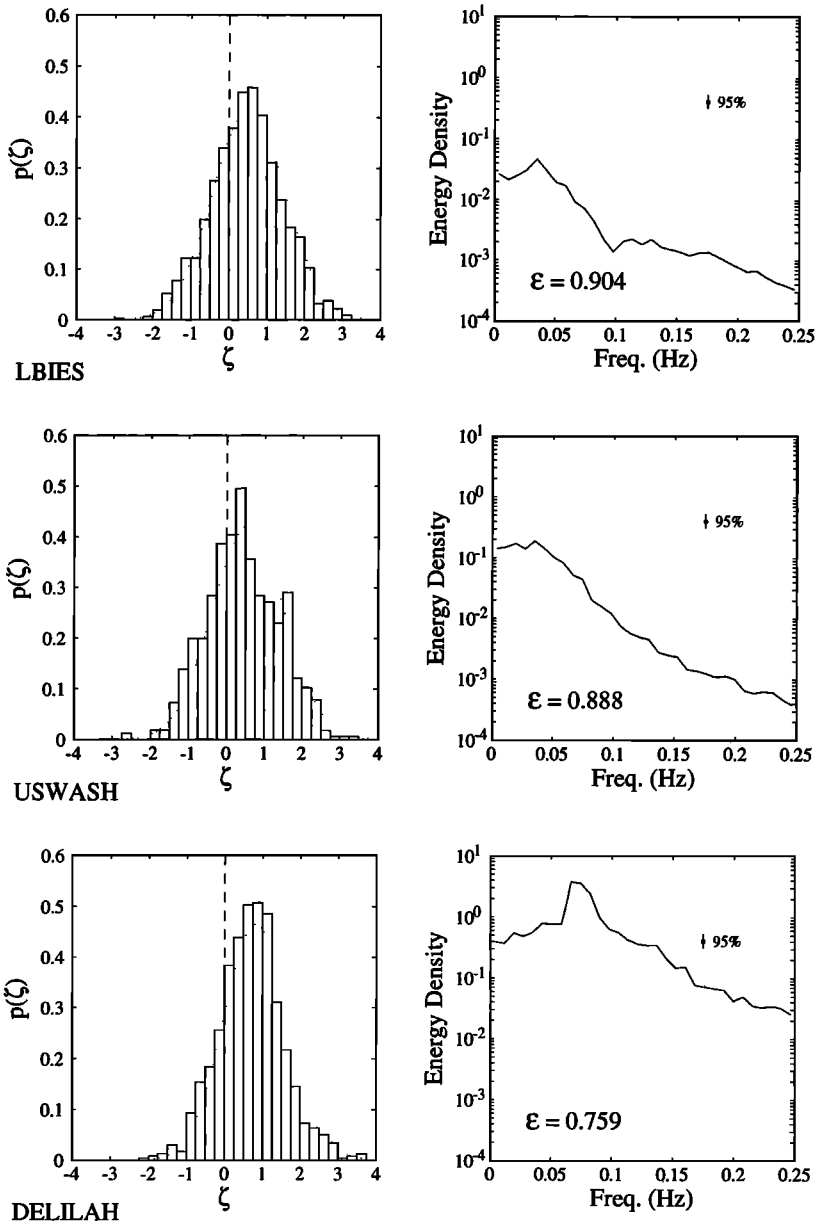

Fig. 4. Example maxima distributions and power spectra from the (top) LBIES, (middle) USWASH, and (bottom) DELILAH experiments. Theoretical distributions for the corresponding spectral width values are shown as the dotted lines. As the spectral width decreases, the proportion of negative maxima (left of the dashed line $\zeta = 0$) decreases in agreement with Figure 2. Energy density units are m^2 per Hz.

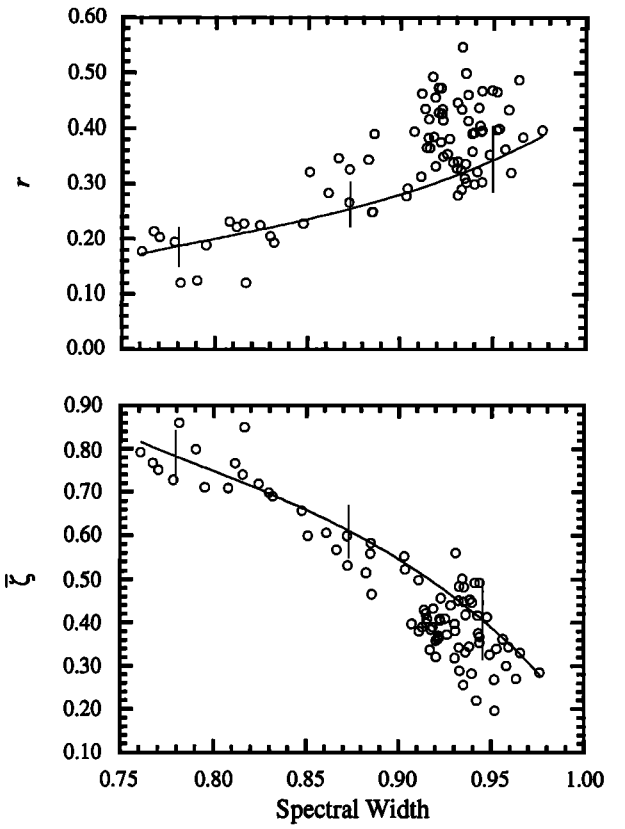

Fig. 5. Statistical measures of (top) r, the fraction of negative maxima, and (bottom) ζ, the mean maximum, as a function of spectral width. Theoretical results formulated using equation (3) are shown as the solid line, with expected ranges found using simulations indicated.

Data were also subjected to a run test [*Bendat and Piersol*, 1986] to verify stationarity such that runs showing trends inconsistent with random fluctuations were removed from the analysis set. Visual examination of each the excluded records confirms that removal was justified on the basis of instrument malfunction or abrupt changes in environmental conditions.

Ultimately, 85 time series were selected. In each case the data were sampled at 2 Hz, with a record length of approximately 2 hours giving a total of 14,336 data points. As low-frequency trends in the time series would severely bias distribution results, all data were quadratically detrended to remove any tidal fluctuations and the wave-induced setup, leaving only the swash signal. In addition, an low-pass filter was applied to eliminate signals having periods shorter than 3 s. The 3-s period was determined using the timestacks to be optimal for isolating maxima visible in the swash signal and restricting maxima due to "noise" in the digitization. Spectral parameters required in the model are determined from smoothed versions of the measured spectra calculated with 112 degrees of freedom. Maxima are defined as having a zero first derivative, and a second-derivative value less than zero. All distributions and distribution statistics pertain to maxima normalized by $\sqrt{m_0}$.

In order to isolate the effect of possible nonlinearities in the data, synthetic, linear time series were constructed by inverse Fourier transforming the observed spectrum, but with randomly selected Fourier phases, ϕ_n. This operation produces a linear simulated time series (given by equation (2)) with identical model input parameters to the original time series. A total of 1000 independent, realizations were produced for each observed swash time series, with appropriate statistics being computed in the same manner as the field data.

Results

Distributions of Swash Maxima

Example probability distributions of swash maxima, ζ, and associated spectra from the LBIES, USWASH, and DELILAH experiments are shown in Figure 4. The theoretical probability density functions estimated using (3) are also shown. For these examples, the agreement between the model and swash maxima observations appears qualitatively reasonable. Note the trend in the observations that as the spectral width increases, the proportion of negative maxima increases in agreement with the theory. The example spectra indicate significant energy is present throughout the incident and infragravity frequency bands. For the complete data set, spectral width values ranged between 0.76 and 0.98, signifying that the data are indeed broad-banded. Clearly, statistical inferences that depend upon a narrow-banded assumption are unjustified for these data.

We quantitatively assessed the model predictions for the observed maxima distribution shapes by applying Monte Carlo type tests using the simulated data. With the simulations serving as the ensemble, parameters describing the fit of the maxima distribution to the CLH56 model (for a specific spectral width value) were computed for each of the 1000 simulations and compared with the actual deviation value obtained using the field data. Using this method, 75 of the 85 runs were observed to have significantly large (greater than 95% of the corresponding simulations) deviation statistics, indicating that the observed and predicted maxima distributions are statistically different. Statistical dissimilarity could not be proven for the remaining 10 runs.

Although the observed and predicted distributions are not statistically equivalent, certain statistics describing the general form of the maxima distributions can be shown to depend upon the model parameter ε. Figure 5 shows plots of ε versus the proportion of negative maxima and the average value of the swash maxima, denoted by r and $\bar{\zeta}$ respectively. Theoretical results are also shown. By examining Figure 5 we see that as spectral width increases, the proportion of negative maxima significantly increases, and the mean maximum significantly decreases, both consistent with model expectations. The agreement between the model and observations for these two bulk statistics is considerable, especially at the lower spectral width values, although the model tends to underpredict r and overpredict $\bar{\zeta}$ for $\varepsilon > 0.9$.

In addition to the more integrated statistics describing the general form of the maxima distributions, probability of exceedance values describing the upper tail of the distribution were also calculated and are shown to be a function of ε. Figure 6 shows plots of ε versus the elevations at which 33, 10, and 2% of the normalized swash maxima were exceeded, denoted $\zeta_{33\%}$, $\zeta_{10\%}$, and $\zeta_{2\%}$, respectively. As in Figure 5, the theoretical results and expected ranges from the simulations are shown. For each statistic, the CLH56 theory predicts that as the spectral width increases, the area under the more positive tail decreases, thereby resulting in lower statistic values. In general the magnitude of the results is appropriate, although the scatter of the $\zeta_{10\%}$ and $\zeta_{2\%}$ results makes identification of any specific trend difficult. Some of the increase in scatter with decreasing α can be attributed to a smaller number of maxima being used in the calculations; however, there does seem to be a consistent bias in the distribution results for $\varepsilon > 0.9$.

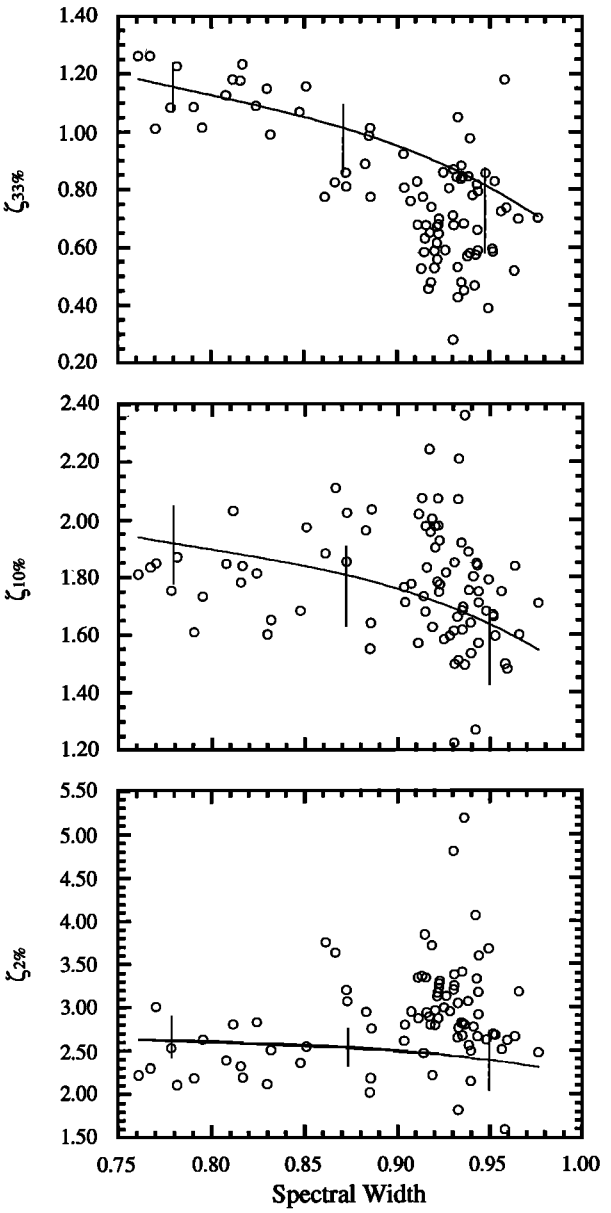

Fig. 6. Exceedance levels as a function of spectral width for probability values (top) 33%, (middle) 10% and (bottom) 2%. Theoretical results and expected ranges are shown as in Figure 5.

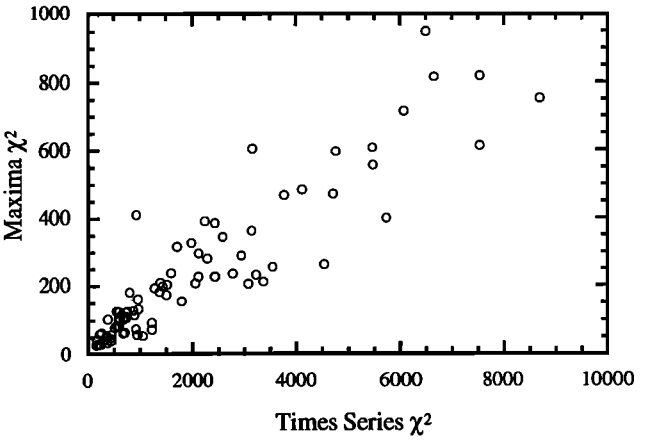

Fig. 7. Chi-square deviation of the swash time series distribution from the Gaussian pdf versus chi-square deviation of the distribution of swash maxima from the CLH56 model pdf.

from the model expectations (Figure 7). Simply put, the more non-Gaussian the swash time series, the farther the model expectations deviate from the maxima observations. A similar relationship exists between the maxima/model chi-square deviation and the skewness of the time series (Figure 8). However, no particular correlation is apparent between the same deviation statistic and either the time series asymmetry, or kurtosis values. Similarly, we found no dependence on either the field site or the sampling method. These results suggest that time series skewness is a useful parameter in expressing deviations of observations from expectations.

Given that nonlinear processes often have nonzero skewness, we can also use the skewness parameter as a reasonable proxy for the degree of time series nonlinearity, and thereby examine the dependence of model performance on the assumption of linear, Gaussian process. The ratio of observed to predicted exceedance values for the $\zeta_{33\%}$, $\zeta_{10\%}$, and $\zeta_{2\%}$ statistics is plotted against the value of time series skewness in Figure 9. We observe that for low skewness values (suggestive of linearity), observed and predicted values are approximately equal, indicating similarity between the model and the observations. However, as skewness (assumed nonlinearity) increases, the data systematically deviates from model predictions. Predicted values of $\zeta_{2\%}$ will underestimate observations if the swash time series has a positive skewness value of

Nonlinearity Results

The most likely explanation of discrepancies between the model and the data is that the fundamental assumption of a linear, Gaussian process is not strictly justified for swash motions. If so, we expect the deviation of the predicted maxima distributions from observations to reflect departures of the swash time series (includes maxima, minima, and all points in between) from the assumed normal distribution as given by various statistical measures.

However, not all of the statistics describing the similarity between the observations and predictions of maxima are affected equally as a function of the various time series "normality" parameters. An expected, straightforward relationship exists between the chi-square deviation of the swash time series from the Gaussian distribution (the fundamental assumption) and the chi-square deviation of the maxima results

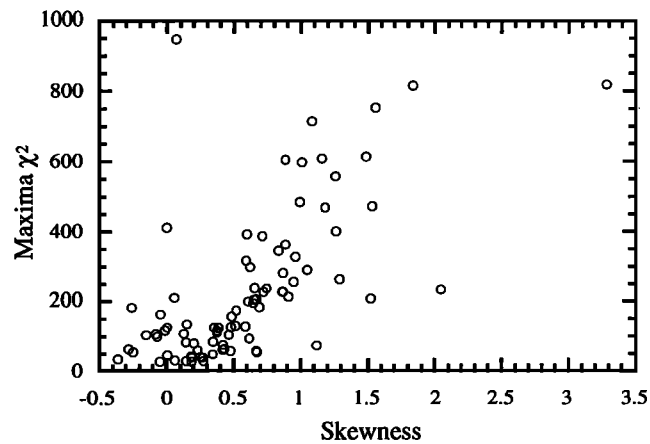

Fig. 8. Chi-square deviation of the distribution of swash maxima from the CLH56 model pdf as a function of time series skewness.

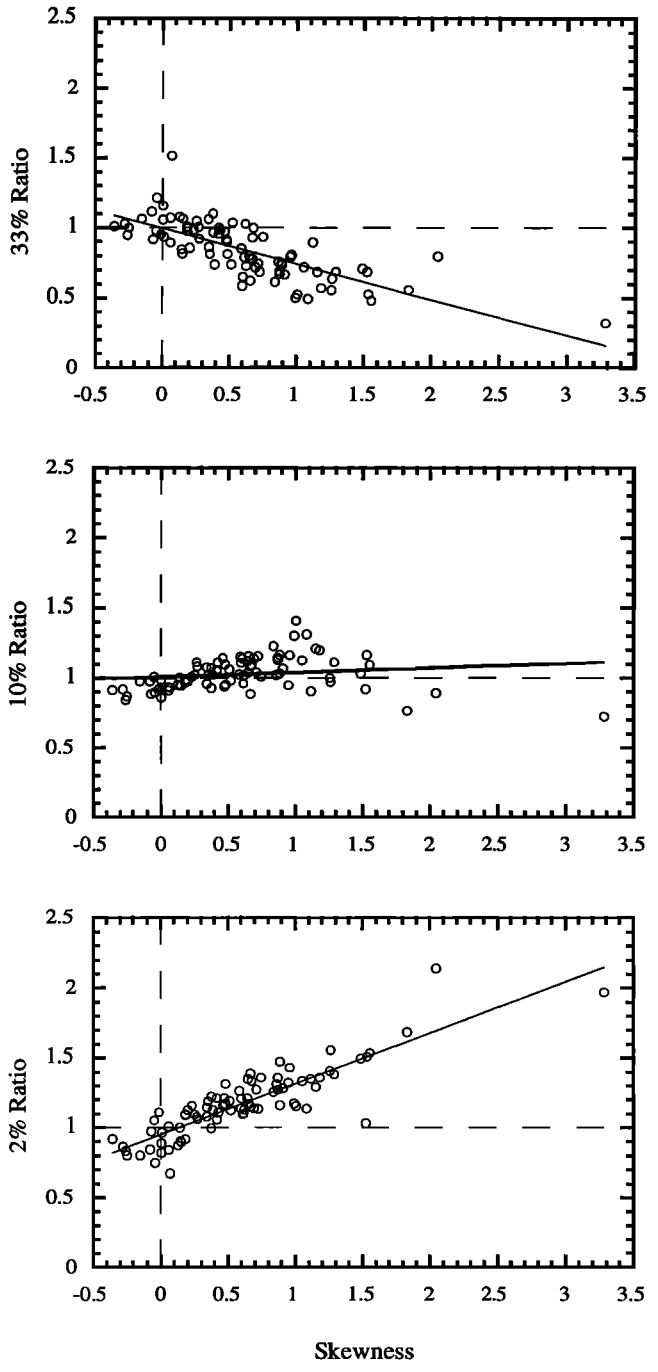

Fig. 9. Ratios of observed to predicted exceedance levels as a function of skewness for probabilities (top) 33%, (middle) 10%, and (bottom) 2%. The intersection of the dashed lines marks the location of expected agreement between the model and observations. The solid line denotes the best linear fit through the data (coefficients given in Table 2).

greater than 0.5. Similar skewnesses will give rise to overestimates of the $\zeta_{33\%}$ observations. However, $\zeta_{10\%}$ ratios have a much smaller dependence on skewness. These trends (which are consistent with the results in Figures 5 and 6) indicate that nonlinearity, as represented by skewness, in the swash time series is being expressed in the distributions of maxima as a shifting of maxima toward the positive extremes (above approximately the ninetieth percentile). Although this shift cannot be accounted for by the linear model, it can be described empirically. The linear trend regression slopes and intercepts of the plots in Figure 9 are given in Table 2.

Discussion

Previously, the distribution of runup maxima has been described in terms of theory that depends upon physically unrealistic energy relationships or empirical weighting coefficients and has often been either directly (for instance, *Nielsen and Hanslow* [1991]) or indirectly (the zero-crossing definition) developed from the assumption of narrow-banded runup spectra. In the preceding sections, swash spectra were shown to be broad-banded rather than narrow-banded with statistics and distributions of maxima clearly dependent upon the relative width of the swash spectral peak. Therefore runup maxima distribution models and statistical formulae dependent upon a peak offshore wave period are almost certainly ill posed. In contrast, functional dependencies between runup maxima and the spectral width parameter are not without precedence. *Van Oorschot and d'Angremond* [1968] suggest that proper application of *Hunt*'s [1989] equation (1) to irregular waves requires a variable proportionality factor, C, that is a function of spectral width. Although it is difficult to relate their findings to our results, both sets of observations support the idea that spectral width has direct implications on the distribution of the runup maxima.

The practical application of the model presented above to wave runup is limited by our present inability to predict the required model parameters and the time series skewness. There are several reasons to suspect the influence of nonlinearity in swash motions including composite sloped beach profiles, bed roughness, permeability, coherent bore-to-bore interactions, and transformation of energy during wave shoaling. The specific influence of any or all of these possible causes is difficult to derive. However, we have demonstrated that various distribution statistics show simple responses to nonlinearity which suggests that future research efforts directed toward improving the predictive capability of the model may prove fruitful. In addition, we hope that our empirical results concerning the trends of extreme runup elevations as a function of nonlinearity are useful for constraining mathematical, nonlinear runup models and for the purposes of nearshore engineering design.

Summary

Runup data from an extensive range of conditions were analyzed to determine if the probability density function of swash maxima could be described using a statistical model based upon the linear superposition of random, Gaussian waves. This model makes no assumptions about the data other than the supposition of a Gaussian process and requires only two input parameters: the spectral width and root-mean-square values of the process of interest. Field data taken under a variety of conditions indicate that although few examples of statistically significant correspondence between the observed maxima distribution and the model pdf were identified, various maxima

TABLE 2. Linear Regression Results Describing Exceedance Ratios as a Function of Skewness

Ratio	Intercept	Slope	R value
33%	0.996	–0.255	0.749
10%	1.009	0.003	0.158
2%	0.995	0.364	0.868

statistics are well parameterized by ε, and that the qualitative trends of the distribution response to changes in ε are appropriate. Quantitatively, discrepancies between observations and predictions varied systematically as a function of time series skewness. Modification of the theory to incorporate nonlinear time series will be necessary to allow more general application.

Acknowledgments. The authors wish to thank the late Paul V. O'Neill for his insight as to the usefulness of the timestack technique and Christine Valentine for performing the majority of the video digitization. Tom Lippmann contributed valuable suggestions which were appreciated. We would like to give special thanks to Bob Guza for providing the runup wire data and helpful comments. The field programs were funded by the Office of Naval Research, Coastal Sciences Program (grants N00014-90-J-1118 and N00014-89-J-1055) and by the U.S. Geological Survey. Data analysis was funded by the U.S. Geological Survey as part of the National Coastal Geology Program.

REFERENCES

Aagaard, T., and J. Holm, Digitization of wave runup using video records, *J. Coastal Res.*, *5*, 547–551, 1989.

Ahrens, J. P., Irregular wave runup, *Coastal Struct. '79*, pp. 998–1019, Am. Soc. of Civ. Eng., New York, 1979.

Ahrens, J. P., Wave runup on idealized structures, *Coastal Struct. '83*, pp. 925–938, Am. Soc. of Civ. Eng., New York, 1983.

Battjes, J. A., Runup distributions of waves breaking on slopes, *J. Waterw., Harbors Coastal Eng. Div. Am. Soc. Civ. Eng.*, *97*, 91–114, 1971.

Bendat, J. S., and A. G. Piersol, *Random Data: Analysis and Measurement Procedures*, John Wiley, New York, 1986.

Birkemeier, W. A., K. K. Hathaway, J. M. Smith, C. F. Baron, and M.W. Leffler, DELILAH experiment: Investigator's summary report, Coastal Eng. Res. Cent., Field Res. Facil., U.S. Eng. Waterw. Exp. Sta., Vicksburg, Miss., 1991.

Carrier, G. F., and H. P. Greenspan, Water waves of finite amplitude on a sloping beach, *J. Fluid Mech.*, *4*, 97–109, 1958.

Cartwright, D. E., and M. S. Longuet-Higgins, The statistical distribution of the maxima of a random function, *Proc. R. Soc. London, Ser. A*, *237*, 212–232, 1956.

Guza, R. T., and E. B. Thornton, Local and shoaled comparisons of sea surface elevations, pressures, and velocities, *J. Geophys. Res.*, *85*(C3), 1524–1530, 1980.

Guza, R. T., and E. B. Thornton, Swash oscillations on a natural beach, *J. Geophys. Res.*, *87*(C1), 483–491, 1982.

Holland, K. T. and R. A. Holman, Measuring runup on a natural beach, II (abstract), *Eos Trans. AGU*, *72*(44), Fall Meeting suppl., 254, 1991.

Holman, R. A., and R. T. Guza, Measuring runup on a natural beach, *Coastal Eng.*, *8*, 129–140, 1984.

Hunt, I. A., Design of seawalls and breakwaters, *Proc. Am. Soc. Civ. Eng.*, *85*, 123–152, 1959.

LeMéhauté, B., B. C. Y. Koh, and L-S. Hwang, A synthesis of wave runup, *J. Waterw. Harbors Div. Am. Soc. Civ. Eng.*, *94*, 77–92, 1968.

Lippmann, T. C., and R. A. Holman, Quantification of sand bar morphology: A video technique based on wave dissipation, *J Geophys. Res.*, *94*(C1), 995–1011, 1989

Miche, R., Le pouvoir réfléchissant des ouvrages maritimes exposés à l'action de la houle, *Ann. Ponts Chausses*, *121*, 285–319, 1951.

Nielsen, P., and D. J. Hanslow, Wave runup distributions on natural beaches, *J. Coastal Res.*, *7*, 1139–1152, 1991.

Rice, S. O., Mathematical analysis of random noise, *Bell Syst. Tech. J.*, *23*, 282–332, 1944.

Rice, S. O., Mathematical analysis of random noise, *Bell Syst. Tech. J.*, *24*, 46–156, 1945.

Sallenger, A. H., S. Penland, S. J. Williams, and J. R. Suter, Louisiana Barrier Island Erosion Study, *Coastal Sediments '87*, pp. 1503–1516, Am. Soc. Civ. Eng., New York, 1987.

Saville, T., Jr., An approximation of the wave runup frequency distribution, Coastal Eng. Conf. Proc. 8th, pp. 48–59, Am. Soc. of Civ. Eng., New York, 1962.

Sawaragi, T., and K. Iwata, A nonlinear model of irregular wave runup height and period distributions on gentle slopes, *Coastal Eng. Conf. Proc. 19th*, pp. 415–434, Am. Soc. of Civ. Eng., New York, 1984.

Suhayda, J. N., Standing waves on beaches, *J. Geophys. Res.*, *79*(21), 3065–3071, 1974.

Thornton, E. B. and R. T. Guza, Energy saturation and phase speeds measured on a natural beach, *J. Geophys. Res.*, *87*(C12), 9499–9508, 1982.

van Oorschot, J. H., and K. d'Angremond, The effect of wave energy spectra on wave runup, *Coastal Eng. Conf. Proc. 11th*, pp. 888–900, Am. Soc. of Civ. Eng., New York, 1968.

K.T. Holland and R.A. Holman, College of Oceanic and Atmospheric Sciences, Oregon State University, Oceanography Administration Building 104, Corvallis, OR 97331-5503.

(Received May 11, 1992;
revised December 31, 1992;
accepted December 31, 1992.)